Article ID: 1000-7032(2012)11-1224-08

Effects of Sputtering Pressure on Microstructure and Chemical Composition of Amorphous $Hg_{1-x}Cd_xTe$ Films

WANG Guang-hua*, KONG Jin-chen,
LI Xiong-jun, YANG Li-li, ZHAO Hui-qiong, JI Rong-bin
(*Kunming Institute of Physics*, *Kunming* 650223, *China*)
* *Corresponding Author*, *E-mail*: *wgh*3068@*yahoo.com*

Abstract: Mercury cadmium telluride films were prepared by RF magnetron sputtering technique at different sputtering pressure on glass substrate. In experiment, X-ray diffraction (XRD), atomic force microscopy (AFM) and energy dispersive spectroscopy (EDS) have been used to characterize the microstructure, surface morphology and chemical composition of $Hg_{1-x}Cd_xTe$ films. Experimental results show that the growth rate, crystal structure, chemical composition content and surface morphology of the $Hg_{1-x}Cd_xTe$ films have a strong relation to the sputtering pressure. When increased the sputtering pressure, the growth rate of films decreased. When the sputtering pressure was more than 1.1 Pa, the prepared $Hg_{1-x}Cd_xTe$ film was amorphous, and when the sputtering pressure was controlled at 0.9 Pa, the films exhibited polycrystalline structure. In addition, the surface roughness (RMS and Ra) of $Hg_{1-x}Cd_xTe$ films gradually decreased with the increasing of sputtering pressure. The chemical composition of films also varing with different sputtering pressure, the Hg and Hg + Cd content in films reache the lowest, but the Cd content gets to the top at 1.1 Pa.

Key words: $Hg_{1-x}Cd_xTe$ films; amorphous semiconductors; microstructure; surface morphology; magnetron sputtering
CLC number: O472.8 **Document code**: A **DOI**: 10.3788/fgxb20123311.1224

溅射气压对非晶 $Hg_{1-x}Cd_xTe$ 薄膜微观结构和化学组分的影响

王光华*, 孔金丞, 李雄军, 杨丽丽, 赵惠琼, 姬荣斌
(昆明物理研究所, 云南 昆明 650223)

摘要: 采用射频磁控溅射制备了非晶态结构的 $Hg_{1-x}Cd_xTe$ 薄膜,并利用台阶仪、XRD、原子力显微镜、EDS 等分析手段对薄膜生长速率、物相、表面形貌、组分比例进行了研究。实验结果表明,溅射气压对薄膜生长速率、微观结构、表面形貌和化学组分有直接影响。随着溅射气压增大,其生长速率逐渐降低。当溅射气压高于 1.1 Pa 时,薄膜 XRD 图谱上没有出现任何特征衍射峰,只是在 $2\theta = 23°$ 附近出现衍射波包,具有明显的非晶态特征;当溅射气压小于 1.1 Pa 时,XRD 谱表现为多晶结构。另外,随着溅射气压的增加,薄膜表面粗糙度逐渐减小,而且溅射气压对薄膜组成的化学计量比有明显影响,当溅射气压为 1.1 Pa 时,薄膜中 Hg 的组分比最低,而 Cd 组分比最高。

关 键 词: 碲镉汞薄膜; 非晶半导体; 微观结构; 表面形貌; 磁控溅射

收稿日期: 2012-07-23; **修订日期**: 2012-09-14
基金项目: 国家自然科学基金(60576069); 国家火炬计划(2011GH011928)资助项目
作者简介: 王光华(1984-), 男, 云南丽江人, 主要从事导体光电材料与器件的研究。
E-mail: wgh3068@yahoo.com.cn, Tel: (0871)5105547

1 Introduction

AII-BIV semiconductors are classical materials used in optoelectronics[1-2], in which $Hg_{1-x}Cd_xTe$ is used in the production of infrared detectors. The main advantage of this material is its electro-optical properties which can be easily changed by varying its composition[3]. The change of the composition of $Hg_{1-x}Cd_xTe$ leads to the change of its energy gap in the range from 0 to a number of eV. In this way, one can design photo-detectors with the maximum of spectra sensitivity expending in the range from visible light to a far infrared[4-6]. Despite the fact that investigations of the solid state solution of $Hg_{1-x}Cd_xTe$ were started in the early 1960s, it is still a non-substituted material. And intensive investigations are being carried out especially in view of the possibility of forming amorphous structure. It has been established that the properties of thin films materials differ significantly from their properties in the bulk form. Similarly, the properties of polycrystalline or crystalline thin films differ markedly from that of amorphous structure[7].

While the amorphous thin film has many features[8], they have a number of interesting physical properties as well as numerous potential applications, such as they can be deposited on any substrates or even directly grow on drive circuit[9]. It is easy to fabricate large area thin films, and there is no limitation of shape. The preparation method of amorphous materials is simple and low cost. They have excellent optical and electrical properties, especially for the photo absorption coefficient[10]. Among all the deposition techniques, the RF magnetron sputtering is one of the best techniques for depositing amorphous or polycrystalline films with high deposition rates at relatively low substrate temperatures. In this technique, the composition of the material is easily controlled. It provides good adherent on large area substrates and control over the physical properties of the deposition films.

The physical properties of the $Hg_{1-x}Cd_xTe$ films are influenced not only by the deposition techniques, but also by some process parameters, such as the target-substrate distance, substrate temperature, sputtering power and sputtering pressure. In this investigation, we have tried RF magnetron sputtering growth of $Hg_{1-x}Cd_xTe$ thin films on glass substrates at different sputtering pressures and researched the effect of sputtering pressure on the quality of amorphous $Hg_{1-x}Cd_xTe$ thin films. The thickness, microstructure, composition and surface morphology of $Hg_{1-x}Cd_xTe$ thin films obtained with different sputtering have been systematically studied.

2 Experiments

A magnetron sputter coating system was used to deposit the $Hg_{1-x}Cd_xTe$ films on the surface of 7105# glasses substrate. A high purity $Hg_{1-x}Cd_xTe$ target was placed below the substrate and the sputtered $Hg_{1-x}Cd_xTe$ particles were deposited on the side of the glass substrate facing the target. The substrate temperature was controlled by water-cooling during the sputtering process. Prior to the growth, the 7105# glass was first immersed in H_2SO_4: $K_2Cr_2O_7$ solution for a few minutes to eliminate oxide, was set in ultrasonic instrument and washed in acetone, ethanol and deionized water for 10 min in succession. After blowing with dry N_2 gas, it was installed into sputtering apparatus. The sputtering chamber was first evacuated to a base pressure of 3×10^4 Pa prior to introducing the high purity argon gas as bombardment gas. During the sputtering, the substrate temperature was controlled at 10 ℃. The target is polycrystalline $Hg_{1-x}Cd_xTe$ and the distance between the substrate and the sources was 50 cm. The shutter located in between the target and the substrate was used to control the sputtering time. In this way, a group of samples were deposited at fixed sputtering power of 30 W and sputtering time of 30 min with different sputtering pressure ranging from 0.9 Pa to 1.5 Pa. The details of sputtering conditions and some experimental results are listed in Table 1.

The corresponding film thickness was determined by surface profiler to evaluate growth rate of $Hg_{1-x}Cd_xTe$ films deposited by RF magnetron sputtering at different sputtering pressure. The phase and structure of

Table 1 The details of sputtering conditions and some experimental results

Sample	Sputtering pressure/ Pa	Thickness/ nm	RMS roughness/ nm	Ra roughness/ nm	Grain size/ nm
A	0.9	672.6	1.748	1.376	35 (220)
B	1.1	591.6	1.545	1.238	–
C	1.3	538.9	1.237	0.999	–
D	1.5	507.0	1.167	0.927	–

$Hg_{1-x}Cd_xTe$ films were tested by XRD technique using D/Max 2200 with Cu Kα ($\lambda = 0.154\ 18$ nm) ray and nickel filter, the diffraction intensity were recorded from 5° to 80° with a step of 0.05°, the working voltage and electricity were controlled at 40 kV and 120 mA, respectively. The surface morphologies and surface roughness of $Hg_{1-x}Cd_xTe$ films were investigated with commercially available atomic force microscopy system (Digital instruments/Veeco dimension 3100) in tapping mode, and the component content of $Hg_{1-x}Cd_xTe$ films was analyzed by EDS using a Phoenix-OIM electron probe microanalyzer (EPMA). All the measurements were performed at room temperature.

3 Results and Discussion

3.1 Growth Rate Analysis

Table 1 provides all the data of film thickness at the different sputtering pressure. Fig. 1 shows the curve of the growth rate of $Hg_{1-x}Cd_xTe$ films deposited at different working pressures. From Fig. 1, it can be seen that with the increase of sputtering pressure from 0.9 to 1.5 Pa, the growth rate of $Hg_{1-x}Cd_xTe$ films decreases gradually from 0.37 to 0.28 nm/s. This trend can be explained as the following reasons. Firstly, the working pressure of system controls mean free path of metastable Ar particles (Ar^*) and sputtering ions (Ar^+). As the working pressure increases, the mean free paths of Ar^* and Ar^+ decrease and then the energy of Ar^+ decreases. Secondly, the mean free paths of Cd, Hg, Te atoms and Cd, Hg, Te ions decrease with the increase of the working pressure. Then the scattering cross section of Cd, Hg, Te particles increases with the working pressure increasing, when the Cd, Hg, Te particles are incident to the growing surface of films[11].

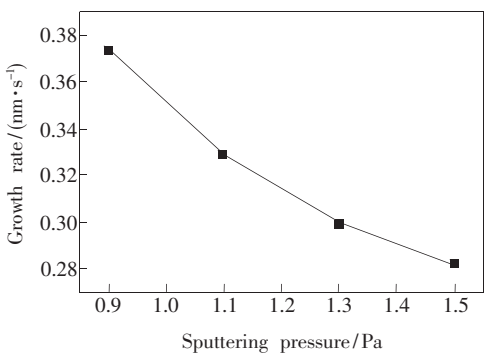

Fig. 1 Relation between the sputtering pressure and growth rate

The films formed at higher sputtering pressures, the mean free path of the sputtering particles is small and the collisions probability is large, when the sputtering particles travel from the target to the substrate. As a consequence, a number of particles is limited and some of the sputtered particles are reflected back to the target[12], which results in the decrease of the deposition rate of films. Similar behavior was observed for CdO films deposited by dc reactive magnetron sputtering[13].

3.2 XRD Analysis

Fig. 2 shows the XRD patterns of $Hg_{1-x}Cd_xTe$ thin films deposited at different pressures. It can be seen that the structure of $Hg_{1-x}Cd_xTe$ films strongly depends on the depositing pressure. The XRD patterns of $Hg_{1-x}Cd_xTe$ films deposited at high pressures (1.1 ~ 1.5 Pa) display no obvious diffraction peak, which means that the structure of materials are amorphous. When the working pressure is decreased from 1.1 to 0.9 Pa, some special diffraction peaks appeared at 23.7°, 39°, 46°, which was as-

signed crystalline $Hg_{1-x}Cd_xTe$ at (111), (220) and (311) preferential orientation. The films formed at low sputtering pressure of 0.9 Pa exhibited polycrystalline. The grain size (d) of the films (220) preferential orientation was calculated from the full width at half maximum intensity of X-ray diffraction peaks using the Scherrer's relation

$$d = \frac{0.9\lambda}{B\cos\theta_B},$$

Where, d is the crystal size, λ is the X-ray wavelength used (Cu Kα, 0.154 nm), B is the full width at half maximum (FWHM) of (220) peak measured in rad, and θ_B is the Bragg angle, we calculated that $d = 35$ nm. The X-ray diffraction studies revealed the optimized sputtering pressure for the growth of amorphous $Hg_{1-x}Cd_xTe$ films.

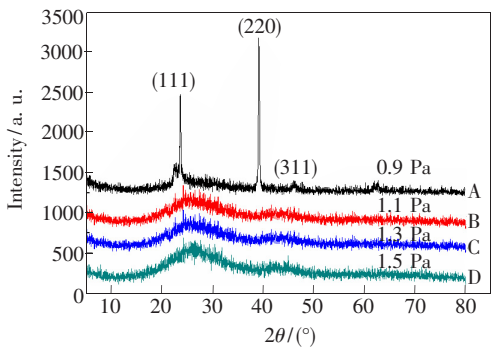

Fig. 2　Comparison of XRD patterns of $Hg_{1-x}Cd_xTe$ films deposited at different Ar pressure

At the sputtering pressure of 1.5 Pa, the mean free path of the sputtering particles is low and the collision between the gas molecules and sputtered atoms is very high. The sputtered atoms arriving at the surface of the substrate have very low kinetic energy. From 1.1 to 0.9 Pa, the kinetic energy of the incident atoms increases. The sputtered particles have enough kinetic energy to arrive at the substrate surface and move to the lowest energy sites and form the low energy structure[14-15]. At the same time, some high-energy gas molecules and sputtered particles bombard the surface of thin films, which increase the roughness of films. The similar behavior was also observed in dc magnetron sputtered TiO_2 films, where highly oriented anatase peak was observed in the films formed at as sputtering pressure of 0.27 Pa[16], in which, the peak width became broader and finally an almost amorphous film was observed with the pressure increased.

3.3　Surface Morphology

AFM measurements were characterized to study surface morphology of $Hg_{1-x}Cd_xTe$ films. Four sets of surface topographies of $Hg_{1-x}Cd_xTe$ films deposited with different sputtering pressure ranging from 0.9 to 1.5 Pa are displayed in Fig. 3 (scanning area is 2 μm × 2 μm). To analyze the surface topographies of $Hg_{1-x}Cd_xTe$ films by digital instruments/veeco dimension 3100 software. There are some significant differences between them, namely, grain size and surface roughness. Fig. 3 (b, c, and d) exhibit a wavy topography created by undulating ridges (ribbons), since obvious crystallization is not observed at higher sputtering pressure, this microstructure feature may be described as an amorphous state. The films are clearly characterized by a hillock-like topography due to circular to elliptical clusters bordered by relatively narrow and deep channels with the width. Every cluster exhibits a substructure of small, dispersed hemispheres, namely a certain number of randomly oriented crystal grains. As the sputtering pressure decreased, as contrasted with the amorphous feature at 1.1, 1.3 and 1.5 Pa, grain features protruding from the film surface occur at lower sputtering pressure. The images in Fig. 3(a) shows random distribution of long columnar shaped grains separated by grain boundaries and some channels, the surface of the $Hg_{1-x}Cd_xTe$ films deposited by RF magnetron sputtering at 0.9 Pa consists of several big grains. While the surface for the $Hg_{1-x}Cd_xTe$ films deposited by RF magnetron sputtering at 1.1, 1.3 and 1.5 Pa show a lot of small uniformly grains, the film surface is smooth and grain size gradually decrease.

From the above discussion, we can found that there are some distinct features during the morphological evolution at the different sputtering pressure in Fig. 3 (a, b, c and d). The feature of the surface topography remaining amorphous at higher sputtering pressure of 1.1, 1.3 and 1.5 Pa and the growth mode tend to epitaxial. When the sputtering pressure was controlled at 0.9 Pa, the transition of

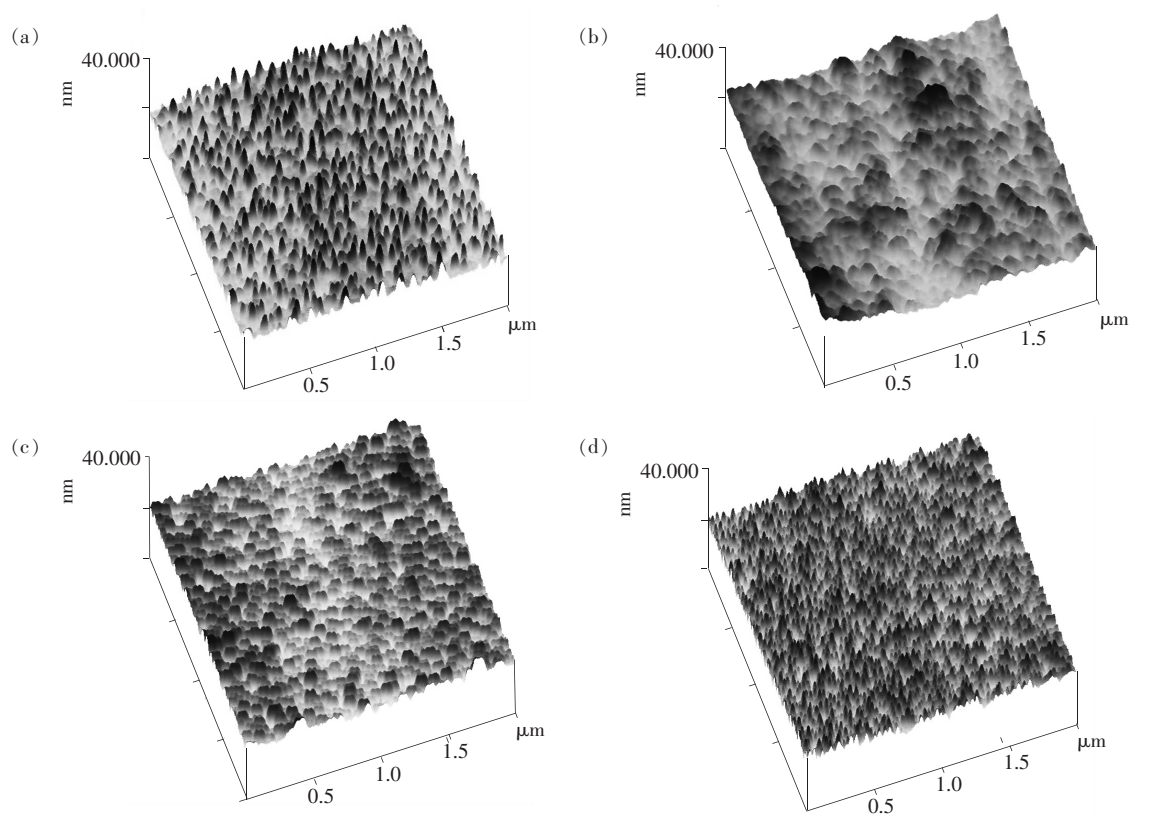

Fig. 3 Atomic force microscopy (AFM) morphological images of $Hg_{1-x}Cd_xTe$ films deposited at different sputtering pressure

grain microstructure from amorphous to crystalline state had happened. We think that these flat parts of the film contain besides amorphous sections granulated (111) or (220) nano-crystallite, which cause the X-ray pattern in Fig. 2(a). These significant changes of surface morphologies are due to the fact that the sputtering pressure affect on the Te-rich growth level and further more affect the atomic mobility on the growing surface and the formation of grains. Generally speaking, in RF sputtering systems, these films are mainly bombarded by sputter neutral target atoms, by reflecting neutral plasma gas atoms, and by sputtering gas ions. When the substrate temperature, incident angle and incident energy remain the same, the intensity of films bombardment is determined by sputtering pressure. The decrease in sputtering pressure results not only in the increase of energy of the particles that bombard the films, but also in increase in amount of deposition atoms arriving to substrate per time unit, which manifests the dependence of deposition rate on sputtering pressure.

To study the surface morphology of $Hg_{1-x}Cd_xTe$ films, it is necessary to measure the main surface roughness parameters of these films, namely RMS, Ra and P-V roughness. Generally, the surface roughness at a certain area is determined by the height differences of all the individual points. RMS roughness is the mean of the root for the deviation from the standard surface to the indicated surface. Ra represents the three-dimensional expansion of the center line mean roughness. In addition, P-V describes the difference between the maximum and minimum values of Z data within the indicated surface or section profile[17-18]. Fig. 4 and Table 1 show the relation between the sputtering pressure and surface roughness (RMS and Ra) of $Hg_{1-x}Cd_xTe$ films as measured over a scan area of 1 μm × 1 μm. Fig. 4 shows that the tendencies of two curves for the increase in sputtering pressure are similar, with the increasing of sputtering pressure, the surface roughness (RMS and Ra) of $Hg_{1-x}Cd_xTe$ films gradually decreased. Now, we take RMS roughness for example to discuss the dependence of the surface roughness parameters on sputtering pressure. At the higher sputtering pressure (above 1.1 Pa), RMS roughness

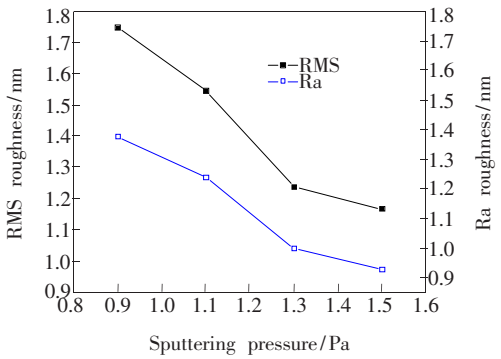

Fig. 4　Relation between sputtering pressure and surface roughness of $Hg_{1-x}Cd_xTe$ films

of $Hg_{1-x}Cd_xTe$ films ranges only from 1.545 to 1.167 nm, related to the formation of amorphous microstructure, as seen in Fig. 2 and Fig. 3 (b, c, d). The shallower deposition Fig. 3 (b, c, d) channels contribute to the smaller surface roughness and lead to the smoother films surface. As grain features occurring at 0.9 Pa in Fig. 3 (a), the formation of the deeper channels results in higher surface roughness of 1.748 nm. These results indicate that the $Hg_{1-x}Cd_xTe$ films grown at 1.1 ~ 1.5 Pa show smooth surface and epitaxial nature.

3.4　Composition Analysis

Fig. 5 and Fig. 6 show the variation of Hg, Cd and Hg + Cd contents in the films obtained at different pressures. With the decrease of the pressure, the chemical composition films changes significantly and the Hg and Hg + Cd content reaches the lowest position, but the Cd content gets to the top at 1.1 Pa.

There are some main reasons leading to the above change[19-20]. The different velocities of different kinds of atoms when they leave the surface of the target, we can deduce the relation of $V(Hg) < V(Te) < V(Cd)$ from the component of $Hg_{1-x}Cd_xTe$ films and target, the collision between the gas molecules and sputtering atoms, and the number of the Hg atoms re-evaporated from the substrate surface which increases with the decrease of the pressure. At high pressure, the kinetic energy of the incident atoms and the mean free path of the sputtering particles are low. All of the sputtered atoms arriving at the substrate will be adsorbed on the surface of the substrate, the number of Hg atoms re-evaporated from the substrate surface is small under this condition, the composition of the films will stay the same or close to the target. With the decrease of the pressure from 1.5 to 1.1 Pa, the collision probability decreases. As is known, the greater the velocity of atoms is, the greater the resistance is. Consequently, the kinetic energy of Hg atoms is more than that of Cd and Te atoms when they arrive at the substrate surface at the same time. Some Hg atoms are re-sputtered, while Cd and Te atoms are left on the substrate. So the composition of Hg in the films becomes lower. When the pressure is decreased from 1.1 to 0.9 Pa, the kinetic energy of sputtered atoms further increases. As they arrive at the substrate, the difference in the kinetic energy between Hg and Cd atoms decreases. Some Cd atoms and Hg atoms are re-sputtered at the same time. The value Hg + Cd of the $Hg_{1-x}Cd_xTe$ films increases with the decrease of the pressure in this range, and the rich-Te phenomena decrease. But it is also lower than

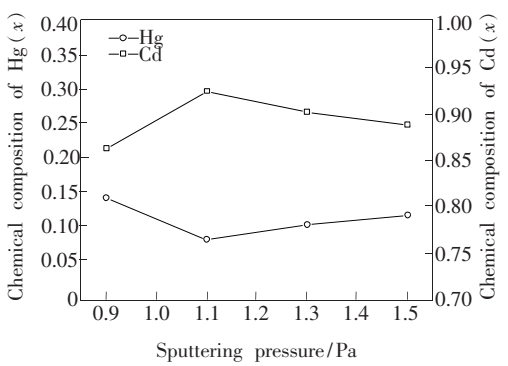

Fig. 5　Composition variation of Hg, Cd with pressure for $Hg_{1-x}Cd_xTe$ film by RF magnetron sputtering at different sputtering pressure on glass substrate

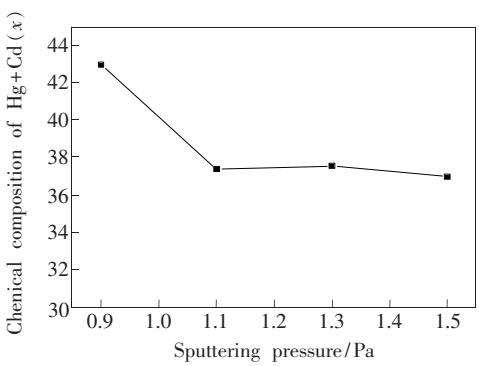

Fig. 6　Composition variation of Hg + Cd with pressure for $Hg_{1-x}Cd_xTe$ films by RF magnetron sputtering at different sputtering pressure on glass substrate

that of the target because the vapor tension of Hg becomes even lower at the same time.

4 Conclusion

In experiment, the $Hg_{1-x}Cd_xTe$ films were deposited on glass substrates using RF magnetron sputtering technique at sputtering pressures ranging 0.9 to 1.5 Pa in keeping the other deposition parameters such as target-substrate distance, sputtering power and substrate temperature as constant. It was observed that the sputtering pressure strongly influenced the properties of the films. with the sputtering pressure increasing, the growth rate of $Hg_{1-x}Cd_xTe$ films decreased, when the sputtering pressure were higher than 1.1 Pa, the $Hg_{1-x}Cd_xTe$ films prepared are amorphous. Films deposited at different sputtering pressure were found to have characteristically different formations and surface morphologies, as observed through atomic force microscopy (AFM), the feature of the surface topography remaining amorphous at higher sputtering pressure and the growth tendency are epitaxial. When the sputtering pressure was controlled at 0.9 Pa, the transition of grain microstructure from amorphous to crystalline state had happened, in this condition the amorphous and crystalline state can be found, the surface roughness (RMS and Ra) of $Hg_{1-x}Cd_xTe$ films gradually decreased with the increasing of sputtering pressure, the chemical composition of films changes significantly and the Hg and Hg + Cd content reaches the lowest, but the Cd content gets to the top at 1.1 Pa.

References:

[1] Rogalski A. Toward third generation HgCdTe infrared detectors [J]. *J. Alloys. Comp.*, 2004, 371(1):53-57.

[2] Rogalski A. Infrared detectors: An overview [J]. *Infrared Phys. Technol.*, 2002, 43(3):187-210.

[3] Guo L, Zhao D X, Zhang Z Z, *et al.* Optoelectronic properties of ZnO/Ag/ZnO multiple films [J]. *Chin. J. Lumin.* (发光学报), 2011, 32(9):920-923 (in Chinese).

[4] Maxey C D, Capper P, Whiffen P A C, *et al.* High-quality p-type $Hg_{1-x}Cd_xTe$ prepared by metalorganic chemical vapor deposition [J]. *Appl. Phys. Lett.*, 1995, 67(23):3450-1-3.

[5] Gopal V, Ashokan R, Dhar V. Compositional characterization of HgCdTe epilayers by infrared transmission [J]. *Infrared Phys.*, 1992, 33(1):39-45.

[6] He L, Chen L, Wu Y, *et al.* MBE HgCdTe on Si and GaAs substrates [J]. *J. Cryst. Growth*, 2007, 301-302:268-272.

[7] Bajaj J. HgCdTe infrared detectors and focal plane arrays [J]. *IEEE*, 1999:23-31.

[8] Jiang D Y, Zhang J Y, Shan C X, *et al.* Solar-blind photodetector based on MgZnO thin films [J]. *Chin. J. Lumin.* (发光学报), 2008, 29(4):743-746 (in Chinese).

[9] Kong J C, Kong L D, Zhao J, *et al.* Structural and optical properties of amorphous MCT films deposited by magnetron sputtering [J]. *J. Semiconductors* (半导体学报), 2008, 29(4):732-736 (in Chinese).

[10] Zhong Z, Sun L J, Xu X Q, *et al.* Effect of high temperature annealing in nitrogen on the luminescence property of ZnO films [J]. *Chin. J. Lumin.* (发光学报), 2010, 31(3):359-363 (in Chinese).

[11] Tang W Z. *The Theory and Technology of the Thin Film Production* [M]. Beijing: Melallurgical Industry Press, 2003: 131-134.

[12] Liu M, Man B Y, Lin X C, *et al.* The effect of incident laser energy on pulsed laser deposition of HgCdTe films [J]. *J. Cryst. Growth*, 2009, 311(4):1087-1090.

[13] Chandramohan S, Sathyamoorthy R, Lalitha S, *et al.* Structural properties of CdTe thin films on different substrates [J]. *Solar Energy Mater. & Solar Cells*, 2006, 90(6):686-693.

[14] Garg A, Kapoor A, Tripathi K N, *et al.* Laser induced damage studies in mercury cadmium telluride [J]. *Opt. Laser Technol.*, 2007, 39(7):1319-1327.

[15] Wang X J, Song H, Li D B, *et al.* Study of AlN films doped by Si thermal diffusion [J]. *Chin. J. Lumin.* (发光学报), 2012, 33(7):769-733 (in Chinese).

[16] Zhu S, Ryu Y, White H W, *et al.* Effects of ambient pressure in pulsed laser deposition morphology and composition study

of epitaxial ZnSe film [J]. *Appl. Surf. Sci.*, 1998, 129:584-588.

[17] Khandelwal R, Singh A P, Kapoor A. Effects of deposition temperature on the structural and morphological properties of thin ZnO films fabricated by pulsed laser deposition [J]. *Opt. Laser Technol.*, 2008, 40(2):247-251.

[18] Reddy A S, Uthanna S, Reddy P S. Properties of DC magnetron sputtered Cu_2O films prepared at different sputtering pressures [J]. *Appl. Surf. Sci.*, 2007, 253(12):5287-5292.

[19] Ma Q B, Ye Z Z. Effects of deposition pressure on the properties of transparent conductive ZnO: Ga films prepared by DC reactive magnetron sputtering [J]. *Mater. Sci. in Semicon. Proc.*, 2007, 10(4):167-172.

[20] Liu M, Man B Y, Lin X C. The effect of substrate material on pulsed laser deposition of HgCdTe films [J]. *Appl. Surf. Sci.*, 2009, 255(9):4848-4851.